Initial Stages of Aggregation in Aqueous Solutions of Ionic Liquids: Molecular Dynamics Studies

B. L. Bhargava* and Michael L. Klein

Center for Molecular Modeling, Department of Chemistry, University of Pennsylvania, 231 South 34th Street, Philadelphia, Pennsylvania 19104-6323

Received: April 17, 2009

Structures formed by 1-alkyl-3-methylimidazolium bromide aqueous solutions with decyl, dodecyl, tetradecyl, and hexadecyl chains have been studied using molecular dynamics (MD) simulations. Spontaneous self-assembly of the amphiphilic cations to form quasi-spherical polydisperse aggregates has been observed in all of the systems, with the size and nature of the aggregates varying with chain length. In all systems, the cation alkyl tails are buried deep inside the aggregates with the polar imidazolium group exposed to exploit the favorable interactions with water. Aggregation numbers steadily increase with the chain length. The hexadecyl aggregates have the most ordered internal structure of the systems studied, and the alkyl chains in these cations show the least number of gauche defects.

1. Introduction

Over the past decade, room temperature ionic liquids (RTILs) have received steadily increasing attention due to their special properties[1−3] and potential for applications.[4−6] These compounds have been extensively investigated using experimental[7,8] and computational methods.[9−14] Binary and ternary mixtures of RTILs have also been studied.[15−19] Apart from these neat mixtures, aqueous solutions of water miscible ionic liquids (ILs) have also attracted significant interest from the scientific community.[20−23] Usually, the ILs with anions such as halides, tetrafluoroborate, or nitrate are water-soluble. Aqueous solutions of imidazolium cationic compounds[22,24] form micelles at a significantly lower concentration compared to alkyltrimethylammonium bromides containing similar length alkyl chains.[25]

The 1-*n*-alkyl-3-methylimidazolium ([$C_n$mim]) cation is amphiphilic by nature with the polar imidazolium group and the nonpolar alkyl tail. In aqueous solution, due to the inherent amphiphilicity, the long alkyl chain substituted compounds should form cationic aggregates. The formation of aggregates depends on the relative strength of Coulombic and hydrophobic van der Waals interactions. Thus, while the compounds with short alkyl chain substituents form isotropic solutions, the ones with longer alkyl chains should form micelles. The self-assembling ability of these compounds can be harnessed to extract products from IL containing systems. It also has several other consequences such as the formation of dispersed or phase-separated systems and in the synthesis and purification of bulk ILs.

Even though there are several experimental studies on aqueous solutions of RTILs,[26−30] there are few theoretical or computational studies.[31,32] Experimental studies usually deal with the critical micelle concentration (CMC), aggregation number, and other macroscopic properties. However, molecular level details can add a great deal to the understanding of these systems, and hence aid in the design of better application-specific ionic liquids.

* To whom correspondence should be addressed. Phone: +1-215-573-8697. Fax: +1-215-573-6233. E-mail: bhargav@sas.upenn.edu (B.L.B.); klein@lrsm.upenn.edu (M.L.K.).

Previous experimental studies suggest that aqueous solutions of RTILs with short alkyl chains (2−4) remain isotropic solutions and the intermediate ones (6−8) form aggregates at very high concentrations. The solutions containing RTILs with longer alkyl chains (>10) form aggregates at very low concentration.[22] There have been several attempts to study the effect of alkyl chain length on the ability of the solution to form aggregates, and to determine the critical aggregation concentration (CAC) and the aggregation number at different concentrations. The various experiments agree on the formation of aggregates with increasing chain length, but the determined aggregation numbers differ widely.[33,22]

We have carried out atomic level molecular dynamics (MD) simulations to gain insights into aggregate formation and the effects of alkyl chain length on aggregate properties. Unfortunately, the complete equilibration of these interesting systems is likely to require simulation trajectories spanning times of the order of microseconds to milliseconds, which is currently not feasible for MD employing all-atom intermolecular interactions. Accordingly, we have focused on the initial (nanosecond) stages of the aggregate formation and not the slower process of aggregate coalescence and equilibration.

2. Methodology and Simulation Details

Classical MD simulations have been carried out on aqueous solutions of a series of 1-*n*-alkyl-3-methylimidazolium bromide ionic liquids using the LAMMPS code[34] and an all-atom force field model developed by Pádua and co-workers.[35] The simple point charge (SPC) model[36] was used for water molecules.

Four different systems of 1-*n*-alkyl-3-methylimidazolium cations with bromide anions were investigated, containing the linear alkyl chains decyl, dodecyl, tetradecyl, and hexadecyl, respectively. The details of the systems studied have been presented in Table 1. Canonical ensemble (NVT) MD simulations were performed following initial MD runs in the isothermal−isobaric (NPT) ensemble to fix the system density. Initial configurations were generated by replicating a monomer in three dimensions and randomly adding water molecules. Three-dimensional periodic boundary conditions were used to

10.1021/jp903560y CCC: $40.75 © 2009 American Chemical Society
Published on Web 06/18/2009

TABLE 1: Details of MD Simulations of [$C_n$mim][Br] Systems, Where *n* is the Length of the Alkyl Chain Substituents

n	no. of ion pairs	no. of water	no. of atoms	run length (ns)	box length (Å)	concn of IL (M)
10	125	7375	27625	30.0	65.4000	0.742
12	125	7407	28471	30.0	66.1676	0.716
14	125	7526	29578	30.0	66.8654	0.694
16	180	7434	33462	30.0	69.2698	0.899

simulate the bulk behavior. Nonbonded interactions were calculated up to a cutoff distance of 13 Å. The potential was not shifted at the cutoff. The particle−particle particle-mesh solver (PPPM) was used to handle long-range electrostatic interactions[37] with an accuracy of 1 part in 10^5. The equations of motion were integrated with a time step of 0.5 fs using the velocity Verlet algorithm. The stretching and bending interactions in the water molecule were constrained using the SHAKE algorithm.[38] Temperature and pressure were controlled via a Nose−Hoover thermostat and barostat with time constants of 1000.0 and 500.0 fs, respectively. The positions of the atoms were stored every 4 ps, and subsequently used for analyses. A binwidth of 0.1 Å is used in the calculation of radial distribution functions (RDFs). Images were rendered using the visualization software VMD.[39]

3. Results and Discussion

3.1. Gauche Distribution. The gauche defect probabilities for torsion around different C−C bonds of the alkyl chains in various [$C_n$mim][Br] aqueous solutions are shown in Figure 1. The graph presents the gauche defect probabilities counting from the headgroup imidazolium ring (H2−H3) to the terminal torsion of the alkyl chain (T3−T2). We can notice from the figure that, for all systems except for the aqueous [C_{16}mim][Br] solution, gauche defect probabilities are highest for T3−T2, which is at the free end of the chain. The other end of the alkyl chain connected to the ring (H2−H3) also shows significant gauche defects and is also the highest in the case of [C_{16}mim][Br]. The defect probabilities are lowest for the bond between the third and fourth carbon atoms from the connected end. However, in the case of the longest alkyl chain studied, the defect concentration decreases further in the middle of the chain. It was observed

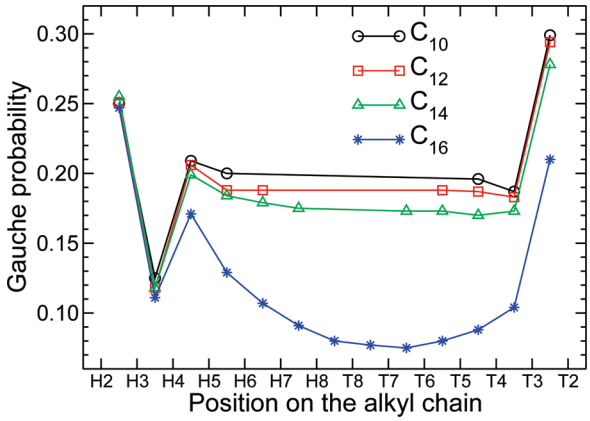

Figure 1. Gauche defect probability for torsion around C−C bonds along the alkyl chain. The *X*-axis gives the positions of alkyl chain C atoms: H2, H3, etc., refer to the second, third, etc., C atoms from the headgroup end, whereas T2, T3, etc., refer to the second, third, etc., C atoms from the tail end. The gauche probability for a particular bond is plotted at the midpoint between the two designated C atoms. Curves in the graph are not fits to the data but are only lines drawn for ease of visualization.

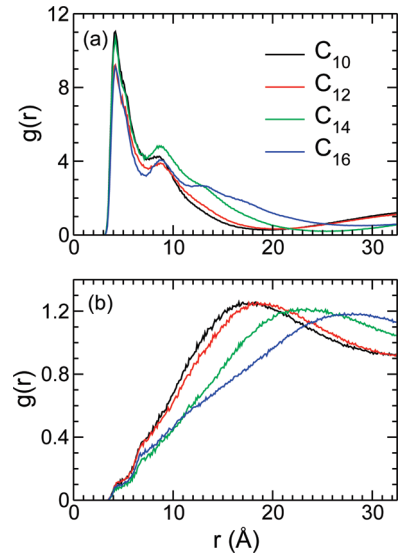

Figure 2. Radial distribution functions for the chain terminal C atom with itself (a) and with bromide anions (b) in aqueous [$C_n$mim][Br] solutions.

that the water penetrates into the aggregates to a certain extent and the straight chain near the ring atoms helps separate the hydrophilic and hydrophobic parts of the cation. The fraction of gauche defects increases as one moves toward the free end of the alkyl chain. It is evident that the longer the alkyl chain length, the lower the probability for gauche defects in the middle of the chain. However, a significant decrease has been observed in the case of [C_{16}mim][Br], which is due to the crystallization of the aggregates to some extent (discussed later). While the decyl, dodecyl, and tetradecyl chains show similar behavior, the hexadecyl chain exhibits a completely different behavior. The significant deviation of the alkyl chains from the all-trans configuration has some effects on the structure of the aggregates formed in the solution.

3.2. Radial Distribution Function. Radial distribution functions (RDFs) provide the probability distribution of atoms around each other. Even though angular information is averaged out in the computation of RDFs, they readily provide significant insights into the structure of the system. RDFs of the terminal carbon atom of the alkyl tails around themselves in all systems studied have been shown in Figure 2a. We can notice that RDFs corresponding to all systems peak at around 4.2 Å and show a small dip near 7.2 Å to show a small hump at 8.8 Å after which each of the peaks show different behavior. All of the RDFs show a narrow peak with amplitude ranging from 9 to 11, suggesting strong organization of the alkyl tails around each other. It was observed that the RDF of head groups of the cations around themselves does not show tall peaks (data not shown). This fact combined with the tail−tail RDFs suggests spatial heterogeneity in these long alkyl chain ionic liquid solutions. It has been observed earlier[40] in the case of pure ionic liquids as well. In aqueous solutions, favorable interaction between the alkyl tails and the unfavorable interactions between these tails and water will lead to the aggregation of cations with their hydrophobic moieties buried inside. While entropic effects prevent the aggregation in solutions of very small chain ionic liquids, the hydrophobic interactions in long alkyl chain aqueous IL solutions predominate and lead to the aggregation. The RDFs in the range between 10 and 20 Å give an estimate of the number of cations belonging to the same aggregate (aggregation number). We can see from the figure that it increases with increasing chain length of the alkyl tail. The RDFs correspond-

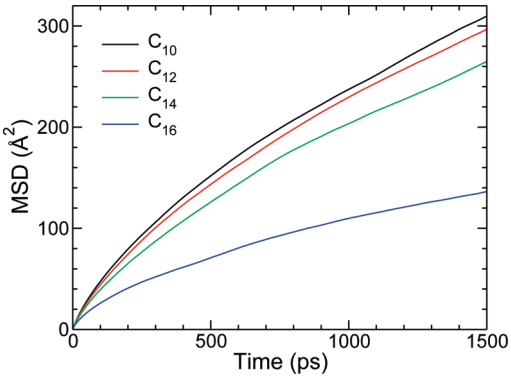

Figure 3. Mean squared displacement of cations of different [$C_n$mim] in aqueous solution. Data are averaged over the last 4 ns of the MD trajectory.

ing to C_{10}, C_{12}, and C_{14} exhibit a minimum around 20 Å; the one corresponding to C_{16} does not show a minimum near that distance. This is due to the larger size of the aggregates present in that system.

Figure 2b shows the radial distribution of anions around the terminal carbon atom of the alkyl chain. Clearly, there are very few anions near the tail end and the first peak for the system with the shortest alkyl chain is around 17 Å. The peak positions for the dodecyl, tetradecyl, and hexadecyl chains are present at 18.5, 23, and 28 Å, respectively. Since the anions are present near the head groups, the peak position of anion−tail RDFs gives an estimate of the size of the aggregates. It is also determined from experiments[22,25] that the aggregation number and hence the size of the aggregates increase with increasing chain length of the alkyl tail. The RDF peaks are very broad and short due to the absence of any direct interaction between the tail and the anions.

3.3. Mean Squared Displacement. The mean squared displacements (MSDs) of cations in different aqueous IL solutions are shown in Figure 3. There are no experimental reports of diffusion coefficients for these systems to compare with. The model is known to typically underestimate the diffusion in pure ILs.[41] However, addition of water accelerates the diffusion of ions due to the electrostatic screening of ions by water.[16] Here, we are only looking at the comparative behavior of diffusion in various solutions differing by the substituent alkyl chain. Anion diffusion is found to be similar in all systems with no noticeable trend in the small variation observed (data not shown). The cation diffusion decreases with the increase in the chain length of the alkyl tail. This behavior is due to the combined effects of two things: the increase in the mass of the cation with the increase in the chain length and the formation of larger aggregates with the increasing chain length. Aqueous [C_{16}mim][Br] solution shows a dramatic change from other systems due to the presence of larger aggregates.

3.4. Formation of Aggregates. Aggregates were observed in all of the systems studied. Cationic oligomers form immediately, and grow by adsorption of monomers. After about 10 ns, aggregates appear to be in a metastable state. Over the next 20 ns of MD simulations, the size of the aggregates did not change noticeably. The cation aggregation in different systems is shown in Figure 4. Notice that the number of aggregates decreases as the length of the alkyl chain on the cation increases. While the [C_{10}mim][Br] solution contains many monomers and oligomers, the [C_{12}mim][Br] system contains relatively few monomers. In the [C_{14}mim][Br] system, most of the cations are part of bigger aggregates, which are larger than those of the systems with smaller alkyl chains. In [C_{16}mim][Br] solution, one can notice one big aggregate and few smaller aggregates. In this case, the size of the simulation system is not large enough to get a statistically significant distribution for the aggregates. Most of the cations in the system can be found to be part of the single large aggregate and the remaining cations form three small aggregates. The increase in the size of the aggregates with the length of alkyl chain is also observed in experimental studies.[25,33]

Contributions to the total intermolecular potential energy arising from the different terms, including the self- and cross-interactions between the head-groups, tails, anions, and water, were computed as a function of time. It was observed that, while the electrostatic energy did not change significantly, there was a large change in the van der Waals energy for tail−tail interactions. The latter also increases with the chain length, as expected. On the basis of the analyses of these pair energies, we assert that the favorable van der Waals interaction between the alkyl tails is responsible for the aggregation of cations in these solutions.

The aggregation numbers and structure of the aggregates were observed to be quite different from each other for differing lengths of the alkyl chain substituent on the cation, which will be discussed below.

3.5. Aggregation Number. The distribution of cations in the system into aggregates of different sizes is shown in Figure 5. In the figures, the fraction of cations involved in the formation of aggregates of size *N* is shown at point *N* along the *X*-axis. Two cations are considered part of an aggregate when the distance between the terminal carbon atoms of their alkyl chain is less than a cutoff distance of 10.5 Å. This distance was chosen after careful visualization of the systems. The aggregation numbers were dependent on the cutoff distance for the [C_{10}mim][Br] system and to a small extent for the [C_{12}mim][Br] system but were not affecting the aggregation number in other systems. In the case of decylmethylimidazolium bromide solution, we can see that most of the cations are involved in the formation of aggregates of a size around 17 and 27. Clearly, the aggregates are polydisperse. There are also few monomers or oligomers of a size between 7 and 11. Note that these are the aggregation numbers at the end of 30 ns. The results are very similar to the ones observed in our previous studies[31] started from a completely different initial configuration. Our previous results were reported after 10 ns of MD simulations. The results after 10 and 30 ns are very similar, suggesting that the system is present in a metastable equilibrium. The complete relaxation of these systems likely requires times of the order of microseconds and thus is not feasible using atomistic simulations with present day computational resources.

In the case of dodecylmethylimidazolium bromide solution, there are only a few aggregate sizes. Most of the cations are present in aggregates of size around 22, but there are other aggregates of size 7, 16, and 19. The small amplitude for the aggregates of size greater than 30 should be noted. These appear on the graph when the small aggregates approach the larger aggregates within the cutoff distance used in the calculation of the aggregation numbers. In the case of tetradecylmethylimidazolium bromide solution, there are only four prominent aggregates with two of them differing only by a single cation. The aggregation numbers observed in this case are 22, 32, and 36. From the figure, we can notice that there are no monomers or oligomers present in the system. For the system with the longest alkyl chain, i.e., hexadecylmethylimidazolium bromide aqueous solution, the results are more dramatic. There is one dominant aggregate whose size is 94 plus two others with sizes

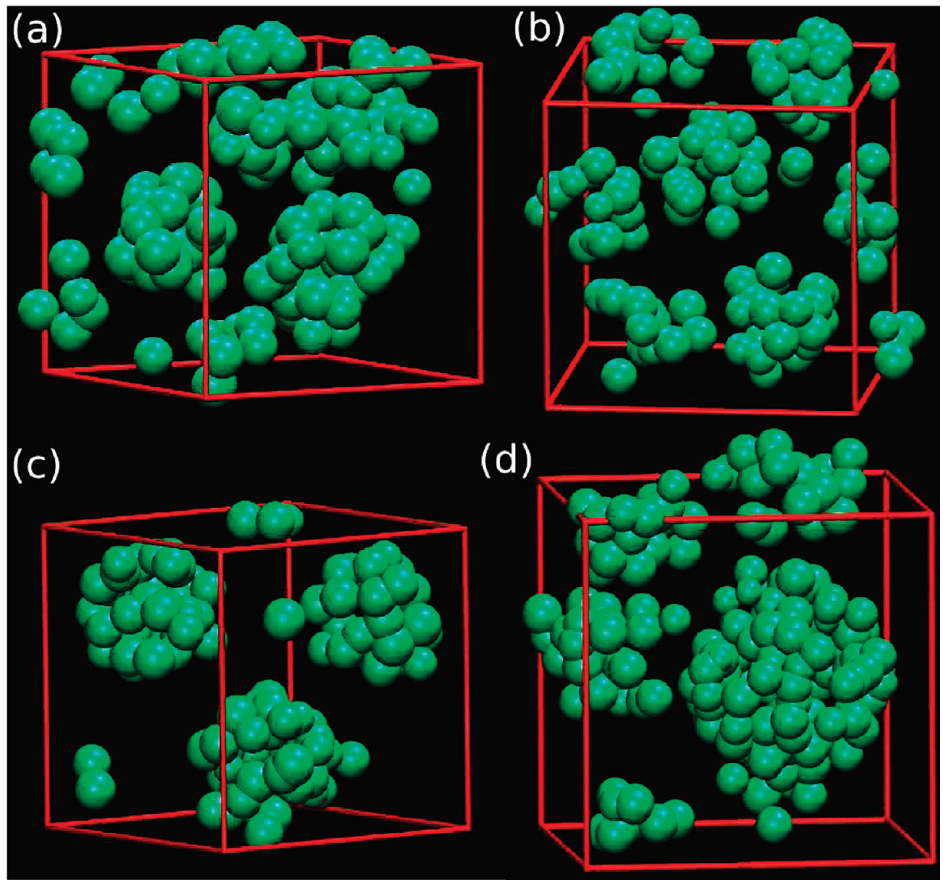

Figure 4. Cationic aggregates in different aqueous [$C_n$mim][Br] solutions at the end of 30 ns MD simulations: (a) [C_{10}mim]; (b) [C_{12}mim]; (c) [C_{14}mim]; (d) [C_{16}mim]. Cations are represented as green beads in the figure. Anions and water are not shown for the ease of visualization.

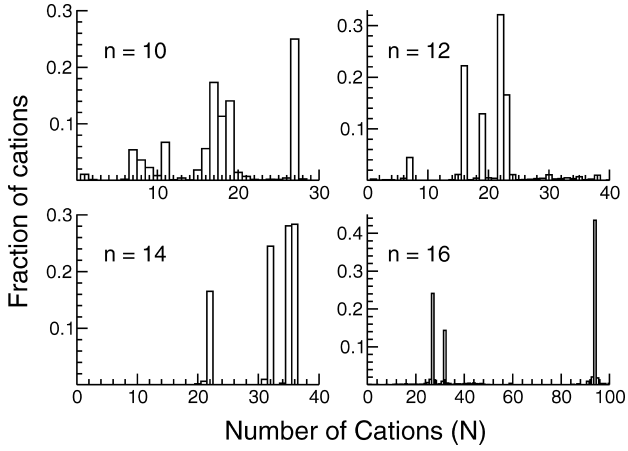

Figure 5. Number of cations involved in forming aggregates of size N for an aqueous solution of [$C_n$mim][Br] for $n = 10$, 12, 14, and 16.

of 27 and 32. Except for the [C_{10}mim][Br], we can see from Figure 5 that the maximum size of the aggregates increases with the increase in the length of the substituent chain. The observed aggregation numbers 27, 22, and 36 for the decyl, dodecyl, and tetradecyl systems, respectively, are smaller than the numbers measured by the static luminescence quenching technique,[25] which are 42, 44, and 59, respectively, for [C_{10}mim][Br], [C_{12}mim][Br], and [C_{14}mim][Br] at lower concentrations. However, the aggregation number for [C_{16}mim][Br], which is 94 as determined from MD simulations, is greater than the experimental value of 66 at a concentration of 0.01 M. The aggregation numbers at higher concentration are expected to be greater than those observed in experiments as in the case of [C_{10}mim][Br] determined from SANS experiments.[33] Atomistic or coarse grained simulations for longer times will be needed to give more accurate values for the aggregation numbers.

The concentration of the aqueous IL solutions studied is much higher than the critical micelle concentration for these systems. Also, the size of the simulation box (number of monomers) employed is not large enough to deal with dilute solutions and hence the statistical uncertainty in the aggregation numbers is significant. For [C_{16}mim][Br] solution, it is clear that the aggregation numbers are so high that in the present system only one proper aggregate can be formed. The objective of the present study is thus to look at the short time behavior of these IL solutions. The results from these studies can be used in improving existing coarse grain models,[32] which can be used to study the long time behavior using considerably bigger systems to obtain statistically more significant aggregation numbers and also the structure of the aggregates closer to equilibrium. Apart from the increase in the aggregation numbers with the increase in the length of the alkyl chain substituent, we observe significant differences in the structure of these aggregates, which is discussed later in this section.

3.6. Structure of Aggregates. The aggregates in all of the systems were found to be quasi-spherical with the hydrophobic alkyl groups buried deep inside the micelles so as to minimize the unfavorable interaction with water molecules. The polar head groups were exposed to water. In [C_{10}mim][Br] and [C_{12}mim]-[Br] solutions, the arrangement of the cation tails within the aggregates was random. We can see from Figure 6a and b, in which the hydrophilic rings and hydrophobic tails are shown in different colors, that the center of the aggregates contains

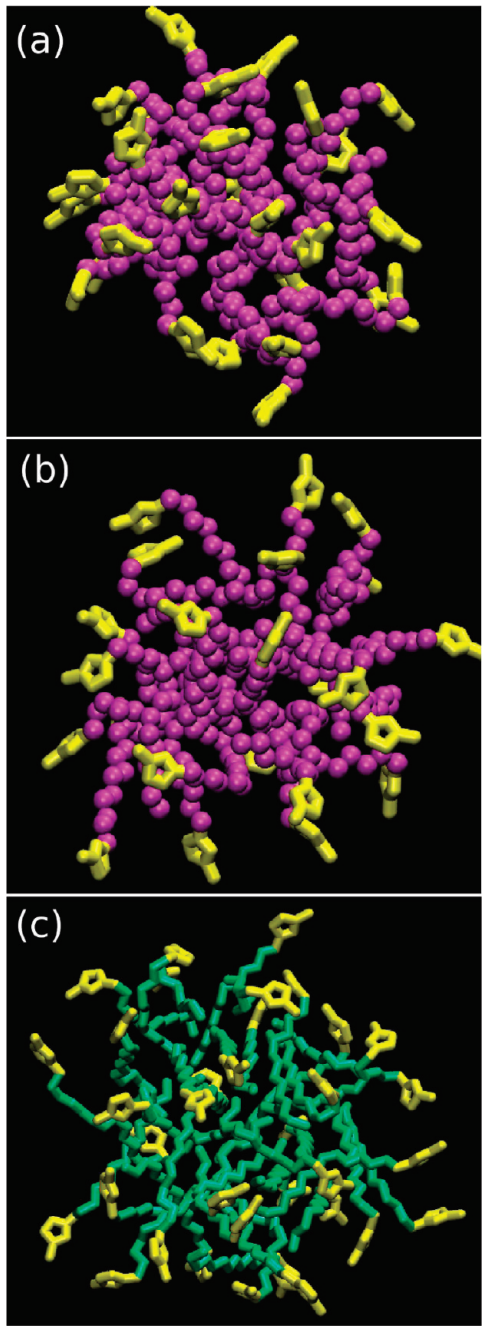

Figure 6. Snapshot of aggregates from various aqueous solutions studied: (a) [C_{10}mim][Br]; (b) [C_{12}mim][Br]; (c) [C_{14}mim][Br]. In parts a and b, atoms belonging to the alkyl tail are represented as magenta spheres and those belonging to headgroup are shown in yellow. In part c, tail group atoms are shown in green and headgroup atoms in yellow. Hydrogen atoms of the cations are not shown. Water molecules, anions, and cations not belonging to the shown aggregate are removed for ease of visualization.

only the alkyl tails. No water molecules or anions were found inside the aggregates. The structure of the aggregates in [C_{10}mim][Br] solution agrees with previous reports.[31] Aqueous [C_{12}mim][Br] solution does not show any significant differences in aggregate structure compared to the [C_{10}mim][Br] solution.

In Figure 6c, the structure of the biggest aggregate in aqueous [C_{14}mim][Br] solution is shown. Only the heavy atoms of the aggregate are shown for the ease of visualization. The polar imidazolium rings can be seen to be present on the surface of the aggregates with tetradecyl chains in the interior region. A small degree of interdigitation of chains can be seen in the figure. The size of the aggregate is also greater than that of the systems with smaller alkyl chains. A snapshot of a part of the aqueous [C_{16}mim][Br] solution is shown in Figure 7. Atoms not belonging to the aggregate and the hydrogen atoms belonging to the aggregate are not shown in the figure for clarity. We can see a near spherical aggregate. However, we can also observe that it is composed of smaller domains of interdigitated cations. Some of the cations are arranged such that their alkyl tails are parallel to each other, allowing for the $\pi-\pi$ interactions between the imidazolium rings. In Figure 7b and c, a snapshot of another micelle in [C_{16}mim][Br] solution is shown in two different views. We can clearly see the interdigitated alkyl chains giving a certain degree of crystallinity to the aggregate. However, the arrangement is not completely crystalline, as we cannot see long-range order.

The probability distributions of the distance between the first and last carbon atoms in the alkyl chain in the aqueous solution of alkylmethylimidazolium bromides are shown in Figure 8. It can be observed from the figure that the distribution becomes broader for the longer alkyl chains due to the increasing possibility of conformations. We can observe a distinct peak at the farther end of each of the distributions, which corresponds to the all-trans conformation. With the increasing chain length, the probability to find an all-trans conformation should rapidly decrease at a given temperature if there are no changes in the structure of the cations. The probabilities to find all-trans conformers are 18.2, 11.6, 8.0, and 26.5%, respectively, for the systems with cations with an alkyl chain substituent of length 10, 12, 14, and 16, respectively. Note the decrease in the probability from decyl to dodecyl to tetradecyl chain systems. The decrease from decyl to dodecyl systems is 6.6%, whereas the decrease from dodecyl to tetradecyl systems is 3.6%. On the basis of the number of different conformations available for the tetradecyl system compared to the dodecyl system, the decrease should have been more. The partial order in these systems is responsible for this behavior. A significant increase in this probability is observed in the hexadecyl system compared with the tetradecyl system. This observation confirms the partial crystallinity of the aggregates in this system, as discussed before.

To summarize, the structure of aggregates in aqueous alkylmethylimidazolium bromide solutions is nearly spherical for the systems varying from decyl to hexadecyl. While the arrangement of the cations with decyl and dodecyl chains is random, the tetradecyl tails show a small degree of order with a few interdigitated alkyl chains. On the other hand, hexadecylmethylimidazolium bromide solutions show a larger degree of crystallinity with domains having either interdigitated or parallel alkyl chains. On the basis of these observations, we expect more crystallinity or liquid crystalline structure for the aggregates in aqueous solutions of higher alkylmethylimidazolium bromide solutions.

4. Conclusions

Room temperature MD simulations have been carried out on a series of long chain 1-*n*-alkyl-3-methylimidazolium bromide aqueous solutions ([$C_n$mim][Br] with n = 10, 12, 14, and 16) at concentrations above the CMC. The cations have been found to self-assemble spontaneously to form aggregates, with the alkyl tails buried inside minimizing unfavorable interactions with water. Headgroup imidazolium rings are present on the surface of the aggregates and exposed to water. Anions and water are not found at the core of the aggregates, though water molecules are found to penetrate to some degree. Analysis of RDFs gives an idea of the shape and size of the aggregates. The system

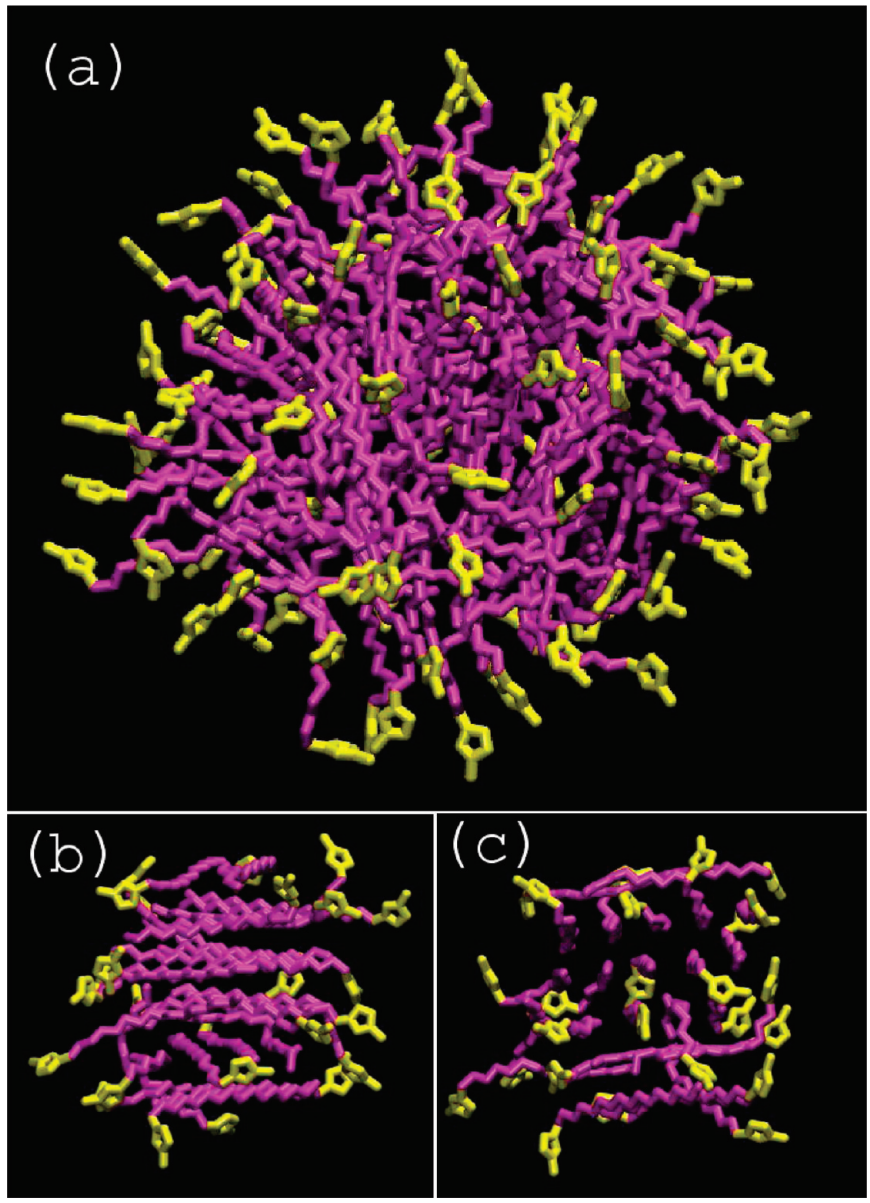

Figure 7. Snapshot of aggregates from aqueous [C_{16}mim][Br] solutions: (a) largest aggregate observed; (b and c) another aggregate from different viewing angles. Tail group atoms are shown in magenta and headgroup atoms in yellow. Hydrogen atoms of the cations are not shown. Water molecules, anions, and cations not belonging to the shown aggregate are removed for ease of visualization.

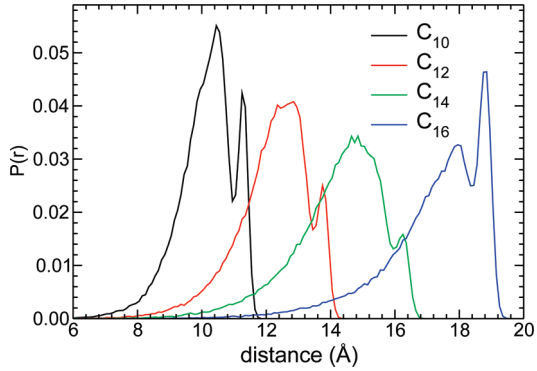

Figure 8. Probability distribution of the distance between the first and last alkyl chain C atoms in aqueous solutions of alkylmethylimidazolium bromide. The data are averaged over the last 4 ns of the MD simulations.

with $n = 16$ shows the least number of gauche defects in its alkyl chains, which is due to the ordered structure they adopt in the aggregates.

Aggregates are quasi-spherical in nature and are polydisperse. One of the aggregation numbers for [C_{10}mim][Br] agrees with experimental NMR studies.[22] The aggregation number increases with the increase in the chain length of the alkyl side chain which is also observed in experimental studies.[25] Cation aggregation is facilitated by the favorable van der Waals interaction between the alkyl tails, and hence, the longer the alkyl tail, the larger are the aggregates. The cation tails within the aggregates in [C_{10}mim][Br] and [C_{12}mim][Br] aqueous solutions are randomly arranged. However, aggregates in [C_{14}mim][Br] show a slight ordering of tails, while those in [C_{16}mim][Br] solution show enhanced ordering. In these ordered aggregates, alkyl tails are either parallel to each other or present in an interdigitated form so as to further increase the favorable interaction. The cations in the aggregates are strongly associated with each other which is evident from the decreased diffusion with increase in the alkyl chain length.

Aggregation is a slow process, likely occurring over a time scale of microseconds or longer. We have followed the time

evolution of these systems for only 30 ns, and therefore, the systems have not evolved to complete equilibrium. The observed aggregation numbers have not changed noticeably over the last 20 ns of the MD run, and thus, the systems have evolved to metastable states. The purpose of this study is to look at the initial stages of aggregation in these systems and the effect of alkyl chains on this process. The aggregation number and the structure of aggregates in [C_{10}mim][Br] solution are very similar to results obtained from previous MD studies started from a completely independent configuration.[31]

The sizes of the systems investigated, though allowing for the formation of a few aggregates, are not large enough to obtain reliable aggregation numbers. For [C_{16}mim][Br] solution, we have observed the aggregation number to be so large that only one proper aggregate was formed in the simulation box. Simulating much larger systems for much longer times is currently unfeasible with present day computational resources. Thus, the results from atomistic simulations such as those reported here should be used to refine the existing coarse grained models[32] to study larger systems and follow them to complete equilibration and get statistically significant values for the aggregation numbers and other properties.

Even with these limitations, on the basis of the observations of the present MD simulations, we predict the structure of aggregates in higher homologues of [$C_n$mim][Br] aqueous solutions to be even more ordered compared to [C_{16}mim][Br] solution. The aggregation number will increase with the increase in alkyl chain length, and the cations might form liquid crystalline or crystalline aggregates in their aqueous solutions.

Acknowledgment. We thank the Ras Al Khaimah Center for Advanced Materials for supporting this work through a research fellowship named for His Highness Sheikh Saqr Bin Mohammed Al Qasimi. Some of the simulations were performed using Teragrid resources.

References and Notes

(1) Tong, J.; Liu, Q.; Xu, W.; Fang, D.; Yang, J. *J. Phys. Chem. B* **2008**, *112*, 4381.
(2) Huddleston, J. G.; Visser, A. E.; Reichert, W. M.; Willauer, H. D.; Broker, G. A.; Rogers, R. D. *Green Chem.* **2001**, *3*, 156.
(3) Wang, Y.; Voth, G. A. *J. Phys. Chem. B* **2006**, *110*, 18601.
(4) Welton, T. *Chem. Rev.* **1999**, *99*, 2071.
(5) van Rantwijk, F.; Sheldon, R. A. *Chem. Rev.* **2007**, *107*, 2757.
(6) Greaves, T. L.; Drummond, C. J. *Chem. Rev.* **2008**, *108*, 206.
(7) Hagiwara, R.; Hirashige, T.; Tsuda, T.; Ito, Y. *J. Fluorine Chem.* **1999**, *99*, 1.
(8) Triolo, A.; Mandanici, A.; Russina, O.; Rodriguez-Mora, V.; Cutroni, M.; Hardacre, C.; Nieuwenhuyzen, M.; Bleif, H.; Keller, L.; Ramos, M. A. *J. Phys. Chem. B* **2006**, *110*, 21357.
(9) Hanke, C. G.; Price, S. L.; Lynden-Bell, R. M. *Mol. Phys.* **2001**, *99*, 801.
(10) Margulis, C. J.; Stern, H. A.; Berne, B. J. *J. Phys. Chem. B* **2002**, *106*, 12017.
(11) Hu, Z.; Margulis, C. J. *Proc. Natl. Acad. Sci. U.S.A.* **2006**, *103*, 831.
(12) Lopes, J. N. A. C.; Pádua, A. A. H. *J. Phys. Chem. B* **2006**, *110*, 7485.
(13) Hunt, P. A. *J. Phys. Chem. B* **2007**, *111*, 4844.
(14) Bhargava, B. L.; Balasubramanian, S.; Klein, M. L. *Chem. Commun.* **2008**, 3339.
(15) Hanke, C. G.; Lynden-Bell, R. M. *J. Phys. Chem. B* **2003**, *107*, 10873.
(16) Kanakubo, M.; Umecky, T.; Hiejima, Y.; Aizawa, T.; Nanjo, H.; Kameda, Y. *J. Phys. Chem. B* **2005**, *109*, 13847.
(17) Bhargava, B. L.; Balasubramanian, S. *J. Phys. Chem. B* **2008**, *112*, 7566.
(18) Inoue, T.; Dong, B.; Zheng, L. *J. Colloid Interface Sci.* **2007**, *307*, 578.
(19) Spickermann, C.; Thar, J.; Lehmann, S. B. C.; Zahn, S.; Hunger, J.; Buchner, R.; Hunt, P. A.; Welton, T.; Kirchner, B. *J. Chem. Phys.* **2008**, *129*, 104505.
(20) Firestone, M. A.; Dzielawa, J. A.; Zapol, P.; Curtiss, L. A.; Seifert, S.; Dietz, M. L. *Langmuir* **2002**, *18*, 7258.
(21) Zhang, H.; Liang, H.; Wang, J.; Li, K. *Z. Phys. Chem.* **2007**, *221*, 1061.
(22) Zhao, Y.; Gao, S.; Wang, J.; Tang, J. *J. Phys. Chem. B* **2008**, *112*, 2031.
(23) Blesic, M.; Lopes, A.; Melo, E.; Petrovski, Z.; Plechkova, N. V.; Lopes, J. N. C.; Seddon, K. R.; Rebelo, L. P. N. *J. Phys. Chem. B* **2008**, *112*, 8645.
(24) Bai, G.; Lopes, A.; Bastos, M. *J. Chem. Thermodyn.* **2008**, *40*, 1509.
(25) Vanyúr, R.; Biczók, L.; Miskolczy, Z. *Colloids Surf., A* **2007**, *299*, 256.
(26) Miskolczy, Z.; Sebők-Nagy, K.; Biczók, L.; Göktürk, S. *Chem. Phys. Lett.* **2004**, *400*, 296.
(27) Bowers, J.; Butts, C. P.; Martin, P. J.; Vergara-Gutierrez, M. C. *Langmuir* **2004**, *20*, 2191.
(28) Blesic, M.; Marques, M. H.; Plechkova, N. V.; Seddon, K. R.; Rebelo, L. P. N.; Lopes, A. *Green Chem.* **2007**, *9*, 481.
(29) El Seoud, O. A.; Pires, P. A. R.; Abdel-Moghny, T.; Bastos, E. L. *J. Colloid Interface Sci.* **2007**, *313*, 296.
(30) Luczak, J.; Hupka, J.; Thöming, J.; Jungnickel, C. *Colloids Surf., A* **2008**, *329*, 125.
(31) Bhargava, B. L.; Klein, M. L. *J. Phys. Chem. A* **2009**, *113*, 1898.
(32) Bhargava, B. L.; Klein, M. L. *Mol. Phys.* **2009**, *107*, 393.
(33) Goodchild, I.; Collier, L.; Millar, S. L.; Prokeš, I.; Lord, J. C. D.; Butts, C. P.; Bowers, J.; Webster, J. R. P.; Heenan, R. K. *J. Colloid Interface Sci.* **2007**, *307*, 455.
(34) Plimpton, S. J. *J. Comput. Phys.* **1995**, *117*, 1. (http://lammps.sandia.gov).
(35) Lopes, J. N. C.; Deschamps, J.; Pádua, A. A. H. *J. Phys. Chem. B* **2004**, *108*, 2038, 11250. Lopes, J. N. C.; Pádua, A. A. H. *J. Phys. Chem. B* **2006**, *110*, 19586.
(36) Berendsen, H. J. C.; Postma, J. P. M.; van Gunsteren, W. F.; Hermans, J. In *Intermolecular Forces*; Pullman, B., Ed.; Reidel: Dordrecht, The Netherlands, 1981; p 331.
(37) Allen, M. P.; Tildesley, D. J. *Computer Simulation of Liquids*; Clarendon: Oxford, U.K., 1987.
(38) Ryckaert, J. P.; Ciccotti, G.; Berendsen, H. J. C. *J. Comput. Phys.* **1977**, *23*, 327.
(39) Humphrey, W.; Dalke, A.; Schulten, K. *J. Mol. Graphics* **1996**, *14*, 33.
(40) Wang, Y.; Voth, G. A. *J. Am. Chem. Soc.* **2005**, *127*, 12192.
(41) Bhargava, B. L.; Balasubramanian, S. *J. Chem. Phys.* **2005**, *123*, 144505. Bhargava, B. L.; Balasubramanian, S. *J. Chem. Phys.* **2006**, *125*, 219901.

JP903560Y